Six- and Five-co-ordinate Ruthenium(II) Complexes with 1,2-Bis(dicyclohexylphosphino)ethane. *X*-Ray Crystal Structure of the d^6 Five-co-ordinate $[RuCl\{(C_6H_{11})_2PCH_2CH_2P(C_6H_{11})_2\}_2]PF_6$

Antonio Mezzetti, Alessandro Del Zotto, and Pierluigi Rigo *
Istituto di Chimica, Università di Udine, V. le Ungheria 43, 33100 Udine, Italy
Nevenka Bresciani Pahor
Dipartimento di Scienze Chimiche, Università di Trieste, P. le Europa 1, 34127 Trieste, Italy

---

Six- and five-co-ordinate complexes of ruthenium(II) with the bulky diphosphine ligand 1,2-bis(dicyclohexylphosphino)ethane (dcpe) have been prepared. In solution, octahedral *trans*-$[RuX_2(dcpe)_2]$ (X = Cl or Br) and *trans*-[RuH(Cl)(dcpe)$_2$] can dissociate giving the unsaturated species $[RuX(dcpe)_2]^+$ and $[RuH(dcpe)_2]^+$, respectively. Phosphorus-31 n.m.r. studies show that the five-co-ordinate d^6 cations, which are stereochemically non-rigid at room temperature, possess a trigonal-bipyramidal geometry with the halide or hydride in an equatorial position. The *X*-ray crystal structure of $[RuCl(dcpe)_2]PF_6$ has been determined: the crystals are monoclinic, space group $P2_1/c$, with $a = 14.614(3)$, $b = 14.625(3)$, $c = 26.196(3)$ Å, $\beta = 100.41(1)°$, and $Z = 4$; final R factor 0.052 for 3 219 observed reflections. The ruthenium cation has an approximate trigonal-bipyramidal geometry, with the bidentate dcpe ligands bridging axial and equatorial postions. This is the first five-co-ordinate complex of ruthenium(II) structurally characterized as trigonal bipyramidal. According to their co-ordinatively unsaturated nature, the complexes $[RuX(dcpe)_2]^+$ react with L (L = CO or MeCN) to form the six-co-ordinate $[RuX(L)(dcpe)_2]^+$, whose stereochemistry and dynamic behaviour were studied by ^{31}P n.m.r. spectroscopy. The influence of the steric properties of the diphosphine on the formation of the $[RuX(dcpe)_2]^+$ species is discussed, and a dominant role for steric effects is suggested.

The co-ordination chemistry of ruthenium(II) complexes with uni- and bi-dentate phosphine ligands has been extensively investigated in recent years.[1] Particular attention has been paid to five-co-ordinated unsaturated species, in view of their relevance in homogeneous catalysis. The major work has been done by Wilkinson and co-workers, who prepared the catalytically active $[RuCl_2(PPh_3)_3]$[2] and $[RuH(Cl)(PPh_3)_3]$.[3] Five-co-ordination in ruthenium(II) complexes containing bidentate phosphines is still relatively uncommon.[4,5] On the contrary, several six-co-ordinate complexes of the type *cis*- or *trans*-$[RuX_2(L\text{–}L)_2]$ (L–L = diphosphine, X = halide) have been obtained with the chelating di(tertiary phosphine) ligands $R_2P(CH_2)_nPR_2$ (n = 1, R = Ph;[6] n = 2, R = Me, Et, or Ph;[6] n = 3, R = Ph[4,5] or Me[7]). However, it is known that with the ligands $Ph_2P(CH_2)_3PPhR$ (R = Ph or Me) the six-co-ordinate complexes *trans*-$[RuX_2(L\text{–}L)_2]$ easily dissociate in polar solvents, giving stable five-co-ordinate $[RuX(L\text{–}L)_2]^+$ cations.[4,5] Also five-co-ordinate $[RuX(L)_2]^+$ cations have been obtained with the six-membered-ring chelate ligand 1-(diphenylphosphino)-2-(2′-pyridyl)ethane,[8] while no five-co-ordinate species can be isolated with the diphosphine $Me_2P(CH_2)_3PMe_2$.[7]

Similar stereochemical effects of the diphosphine alkyl-chain length have been observed in the series *trans*-$[RuH(X)\{Ph_2P(CH_2)_nPPh_2\}_2]$. The five-co-ordinate cations $[RuH\{Ph_2P(CH_2)_nPPh_2\}_2]^+$ can be obtained when n is 3 or 4,[9] but when the size of the chelate ring is reduced the six-co-ordinate solvates $[RuH(solv)\{Ph_2P(CH_2)_nPPh_2\}_2]^+$ (n = 1, solv = H_2O;[10] n = 2, solv = EtOH[9]) are preferentially formed.

The different behaviour of *trans*-$[RuX_2(L\text{–}L)_2]$ with L–L = $R_2P(CH_2)_3PR_2$ (R = Ph or Me) toward dissociation suggests that also the bulkiness of the substituents at phosphorus is an important factor in determining the stability of five-co-ordinated species. With this in mind, we have been investigating a series of ruthenium(II) complexes formed with 1,2-bis(dicyclohexylphosphino)ethane (dcpe), a bidentate phosphine with the sterically demanding end groups $-P(C_6H_{11})_2$. In this paper we report on the syntheses of the six-co-ordinate complexes *trans*-$[RuX_2(dcpe)_2]$ (X = Cl or Br) and *trans*-[RuH(Cl)(dcpe)$_2$], as well as their halide-dissociation products $[RuX(dcpe)_2]BPh_4$ and $[RuH(dcpe)_2]PF_6$, which have been characterized by means of electronic and ^{31}P n.m.r. spectroscopy.

Since solid-state structural data are still relatively rare for five-co-ordinate ruthenium(II) complexes,[1] we have also determined the crystal structure of $[RuCl(dcpe)_2]PF_6$. Theoretical treatments indicate that a square-pyramidal geometry is favoured for the five-co-ordinate d^6 configuration,[11] and in fact all five-co-ordinate ruthenium(II) complexes structurally characterized are satisfactorily described as square pyramids.[12–14] We now find that the $[RuCl(dcpe)_2]^+$ cation is best described as a trigonal bipyramid, with the chlorine in an equatorial position. This is of interest also in view of the controversial interpretation of ^{31}P n.m.r. results in the stereochemical assignment of the $[RuX(L\text{–}L)_2]^+$ species.[5,15] Furthermore, we report on the fluxional behaviour of the compounds $[RuX(L)(dcpe)_2]^+$ (X = Cl or Br; L = CO or MeCN), which is apparently related to a low-temperature restricted motion of the ligands in the sterically crowded six-co-ordinated derivatives.

Results and Discussion

The ligand dcpe reacts with $[RuX_2(dmso)_4]$[16–18] (dmso = dimethyl sulphoxide) in boiling benzene to yield the air-stable

---

† Bis[1,2-bis(dicyclohexylphosphino)ethane]chlororuthenium(II) hexafluorophosphate.

Supplementary data available: see Instructions for Authors, *J. Chem. Soc., Dalton Trans.*, 1989, Issue 1, pp. xvii—xx.

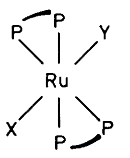

	X	Y
(1)	Cl	Cl
(2)	Br	Br
(3)	H	Cl

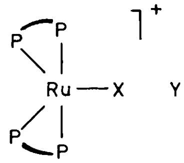

	X	Y
(4)	Cl	BPh$_4$
(5)	Br	BPh$_4$
(6)	I	BPh$_4$
(7)	Cl	PF$_6$
(14)	H	PF$_6$

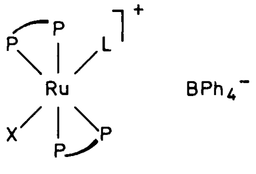

	X	L
(8)	Cl	CO
(9)	Br	CO
(10)	I	CO
(11)	Cl	MeCN
(12)	Br	MeCN
(13)	I	MeCN

Table 1. I.r. and u.v.-visible spectroscopic data

Complex	I.r.[a], $\nu_{max.}$/cm^{-1}	U.v.-visible, $\lambda_{max.}$/nm ($\varepsilon_{max.}$/dm^3 mol^{-1} cm^{-1} for solution)
(1)	300[b]	320 (sh), 460 (93)[c], 330, 450[d]
(2)		340 (sh), 485 (100)[c], 340, 485[d]
(3)	1 985[e]	
(4)		338 (1 920), 460 (990), 555 (940)[f] 340, 455, 555[d]
(5)		340 (sh), 470 (1 010), 565 (978)[f] 350, 465, 560[d]
(6)		340 (sh), 490 (961), 580 (982)[f] 335, 480, 555[d]
(8)	1 940,[g] 280[b]	
(9)	1 940[g]	
(10)	1 940[g]	
(11)	2 244[h]	
(12)	2 248[h]	
(13)	2 254[h]	
(14)	2 150[e,f]	

[a] In Nujol mull, unless otherwise stated. [b] ν(Ru–Cl); not reported when the attribution is uncertain. [c] In benzene solution. [d] In Nujol mull. [e] ν(Ru–H). [f] In dichloromethane solution. [g] ν(CO). [h] ν(CN), in dichloromethane solution.

yellow or pink crystalline diamagnetic *trans*-[RuX$_2$(dcpe)$_2$] [X = Cl (**1**) or Br (**2**)], which can also be conveniently prepared by refluxing [RuX$_2$(PPh$_3$)$_3$] with 2 equivalents of the diphosphine in benzene. The visible spectra of these complexes show, both in the solid state and in solution, a weak absorption in the 460—485 nm region, with a shoulder at higher frequency (Table 1), and closely resemble those of other *trans*-[RuX$_2$(L–L)$_2$] derivatives.[4,5,19] The *trans* geometry of (**1**) and (**2**) can be inferred from their ^{31}P-{^{1}H} n.m.r. spectra in benzene solution, which show a single signal at about 38 p.p.m., in agreement with the presence of four equivalent phosphorus atoms (Table 2). Moreover, the i.r. spectrum of (**1**) exhibits, in the Ru–Cl stretching region, a band at 300 cm^{-1}, which is absent from the spectrum of (**2**), and can therefore be assigned to terminal chlorines in mutually *trans* positions (Table 1).

The reaction of 2 equivalents of dcpe with [RuH(Cl)(PPh$_3$)$_3$] produces white *trans*-[RuH(Cl)(dcpe)$_2$] (**3**), whose i.r. spectrum shows an intense Ru–H absorption at 1 985 cm^{-1}. In the metal–hydride region, the ^{1}H n.m.r. spectrum of (**3**) in benzene solution exhibits a quintet pattern, consistent with coupling to four equivalent phosphorus atoms. The *trans* geometry of (**3**) is also confirmed by the ^{31}P-{^{1}H} n.m.r. spectrum, which shows a single signal at 65.3 p.p.m.

The dissolution of the six-co-ordinate species (**1**)—(**3**) in benzene occurs without apparent structural changes; by contrast, in polar solvents (**2**) and (**3**) dissociate giving rise to conducting solutions, in which ionic species are present. When the pink complex (**2**) is dissolved in dichloromethane a purple solution is formed. The molar conductance for a 10^{-3} mol dm^{-3} solution (Table 3) is near to the typical values of 1 : 1 electrolytes, and its visible spectrum shows the usual features of five-co-ordinate [RuX(L–L)$_2$]$^+$ chromophores, thus suggesting the occurrence of the dissociation (1). Also the hydrido-complex (**3**) is dissociatively unstable in polar solvents, and spectroscopic and conductivity data suggest that dissolution in dichloromethane occurs with the formation of a cationic five-co-ordinate species (Tables 2 and 3). The dichloro derivative (**1**) is insoluble in dichloromethane, and both (**1**) and (**2**) are insoluble in nitromethane and acetonitrile.

$$trans\text{-}[\mathrm{RuX_2(dcpe)_2}] \rightleftharpoons [\mathrm{RuX(dcpe)_2}]^+ + \mathrm{X}^- \quad (1)$$

Co-ordinatively unsaturated [RuX(dcpe)$_2$]$^+$ species can be isolated by two different routes. Treatment of [RuX$_2$(dmso)$_4$] in boiling ethanol with the equivalent amounts of dcpe in the presence of excess of NaBPh$_4$ gives purple diamagnetic crystals analyzing as [RuX(dcpe)$_2$]BPh$_4$ [X = Cl (**4**), Br (**5**), or I (**6**)] (Table 3). Complexes (**4**) and (**5**) can be prepared also by refluxing [RuX$_2$(PPh$_3$)$_3$] (X = Cl or Br) and dcpe in ethanol in the presence of NaBPh$_4$. The formulation of (**4**)—(**6**) as five-co-ordinate species follows from conductivity and spectroscopic data. Their dichloromethane or acetone solutions exhibit conductivity values (Λ_M) in the typical range for 1 : 1 electrolytes containing tetraphenylborate.[20]

To rule out dimeric or polymeric structures containing halide bridges, the conductivities of acetone solutions of complexes (**4**)—(**6**) were measured at different molar concentrations (c), and the molar conductivity Λ_M was plotted against $\sqrt{c}$. The limiting molar conductivity Λ_0 and the Onsager coefficient α, determined according to Onsager equation $\Lambda_0 = \Lambda_M + \alpha\sqrt{c}$, are in good agreement with the values calculated for 1 : 1 electrolytes (Table 3). Complexes (**4**)—(**6**) behave as 1 : 1 electrolytes also in nitromethane and acetonitrile, but the dissolution of the compounds in these solvents is accompanied by a colour change from purple to yellow, which suggests the formation of six-co-ordinate solvates (see below).

The solid-state electronic spectra of (**4**)—(**6**) are very similar to each other, with definite bands at 460—490 and 550—580 nm, and a shoulder at 340 nm. The energies of the maxima produce the usual spectrochemical series I < Br < Cl. The spectral patterns are strictly related to those of other low-spin five-co-ordinate complexes of ruthenium(II) with a P$_4$X donor set.[4,5] The solution spectra are markedly dependent upon the nature of the solvent. Those in dichloromethane or acetone are practically coincident with the solid-state ones, suggesting that no structural rearrangement occurs upon dissolution of the compounds in these solvents.

The ^{31}P n.m.r. spectra of complexes (**4**)—(**6**) were studied over a range of temperatures in dichloromethane or CD_2Cl_2–CHF_2Cl solutions; some spectra of **(4)** at different temperatures are reported in Figure 1. The room-temperature proton-decoupled ^{31}P n.m.r. spectra of the $[RuX(dcpe)_2]^+$ cations in dichloromethane show two broad signals of equal intensity at about 80 and 52 p.p.m. By lowering the temperature, a resolved spectrum is obtained at 263—253 K, which consists of two triplets with a $^2J(P–P)$ of about 16 Hz. As the temperature is lowered below 253 K the two triplets begin to broaden, losing their fine structure. In the range 223—163 K the signals remain broad, with the one at 80 p.p.m. shifting downfield, and at 143 K they are eventually resolved into two triplets, with the lower-frequency resonance sharpening up more rapidly.

The n.m.r. results in the range 310—253 K suggest that five-co-ordinate **(4)**—**(6)** are non-rigid on the n.m.r. time-scale at these temperatures, and become stereochemically rigid at lower temperatures. No other species are present at concentrations detectable by n.m.r. spectroscopy in this temperature range. A similar behaviour has been reported for several five-co-ordinate complexes of the type $[MX(L–L)_2]^{n+}$ (M = d^6 or d^8 metal ion)[5,21,22] for which the doublet of triplets has been interpreted in terms of a trigonal-bipyramidal structure (t.b.p.) with the diphosphine ligands spanning axial and equatorial positions. However, since a square pyramid should be favoured in the case of d^6 metal complexes,[11] the pair of triplets observed in the ^{31}P

Table 2. ^{31}P N.m.r. data[a]

Complex	δ/p.p.m.	J(P–P′)/Hz	T/K
(1)	39.3 (s)		310
(2)	37.3 (s)		310
(3)[b]	65.3 (s)		310
(4)	52, 81[c]		310
	51.8 (t), 83.1 (t)	16.1	253
	51.5 (t), 90.5 (t)	14.6	143
(5)	52, 80[c]		310
	51.9 (t), 81.5 (t)	15.7	253
	51.6 (t), 90.7 (t)	13.2	143
(6)	54.6, 77.4[c]		310
	53.9 (t), 77.8 (t)	16.2	253
	53.6 (t), 85.7 (t)	13.7	143
(8)[d]	48.2 (s)		310
	39.3, 51.6, 61.1, 61.8	15.8, 19.1, 223.5, 227.8, 16.7, 3.4	133
(9)[d]	49.0 (s)		310
	37.6, 49.3, 59.4, 59.8	18.9, 15.8, 228.9, 228.6, 14.2, 6.7	153
(10)[d]	47.3 (s)		310
	36.6, 46.3, 57.2, 57.7	13.0, 18.4, 219.5, 220.0, 17.6, 9.3	153
(11)[e]	43.3 (s)		310
(12)[d]	43.4 (s)		310
	29.4, 40.6, 56.8, 58.8	16.7, 21.7, 243.5, 249.5, 21.2, 5.8	143
(13)[d]	43.0 (s)		310
	29.5, 38.9, 55.5, 57.4	15.3, 21.0, 238.8, 242.2, 20.8, 4.4	153
(14)[f]	60.1[c]		310
	54.6 (t), 69.8 (t)	13.9	213

[a] Solvents used: ^{31}P, CH_2Cl_2 (310—173 K), CHF_2Cl—CD_2Cl_2 (173—133 K); ^1H CD_2Cl_2. Multiplicity given in parentheses: s = singlet, t = triplet, tt = triplet of triplets, and q = quintet. [b] High-field ^1H n.m.r. data (310 K): $\delta = -21.7$ (q), $J(P–H) = 19.5$ Hz. [c] Broad signal. [d] Low-temperature spectra analyzed as ABCD spin systems. The relative signs for $^2J(P–P)$ cannot be unambiguously derived from experimental spectra; simulations performed assuming positive *trans*-$^2J(P–P)$ and negative *cis*-$^2J(P–P)$ constants; calculated spectrum for complex **(10)** is shown in Figure 2. Refined parameters reported in the order: δ(A), δ(B), δ(C), and δ(D); J(AB), J(AC), J(DC), J(BC), J(BD), and J(CD). [e] Low-temperature limiting spectrum not reached at 133 K. [f] High-field ^1H n.m.r. data: $\delta = -5.8$ (q), $J(P–H) = 21.5$ (310 K); -6.0 (tt), $J(P–H) = 30.7$, $J(P'–H) = 10.6$ Hz(213 K).

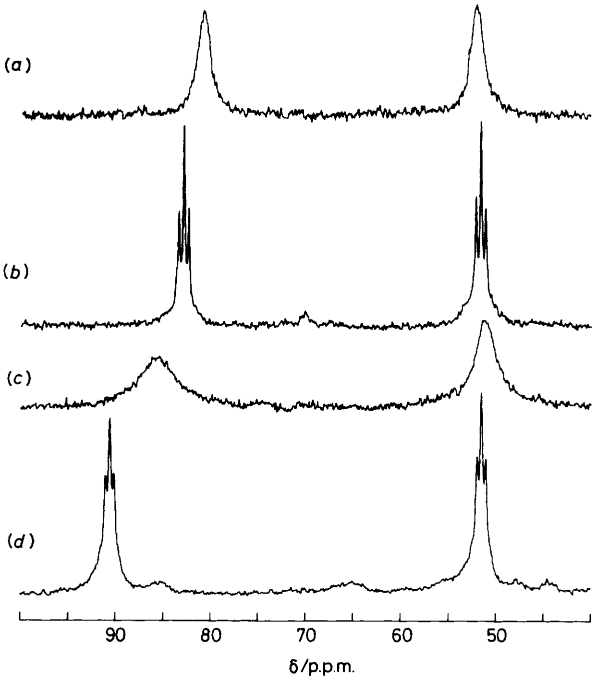

Figure 1. Variable temperature ^{31}P n.m.r. spectra of complex **(4)**: at (*a*) 310, (*b*) 253, (*c*) 193, and (*d*) 143 K

Table 3. Analytical and physical data

	Complex	Colour	M.p. (decomp.) θ/°C	Λ_M[a]/ Ω^{-1} cm^2 mol^{-1}	Analysis (%)[b]	
					C	H
(1)	*trans*-$[RuCl_2(dcpe)_2]$	Pale orange	>250		61.15 (61.40)	9.55 (9.50)
(2)	*trans*-$[RuBr_2(dcpe)_2]$	Pink	>250	36[c]	56.85 (56.45)	8.70 (8.75)
(3)	*trans*-$[RuH(Cl)(dcpe)_2]$	White	>250	35[c]	63.35 (63.55)	10.00 (9.95)
(4)	$[RuCl(dcpe)_2]BPh_4$	Purple-red	133—135	77[d]	69.20 (70.15)	9.00 (9.00)
(5)	$[RuBr(dcpe)_2]BPh_4$	Purple	144—146	82[d]	66.95 (67.85)	8.70 (8.70)
(6)	$[RuI(dcpe)_2]BPh_4$	Purple	180—182	80[d]	64.70 (65.55)	8.45 (8.40)
(7)	$[RuCl(dcpe)_2]PF_6$	Purple-red	218—220	124	55.40 (55.45)	8.70 (8.60)
(8)	*trans*-$[RuCl(CO)(dcpe)_2]BPh_4$	White	189—191	74	68.35 (69.60)	8.80 (8.80)
(9)	*trans*-$[RuBr(CO)(dcpe)_2]BPh_4$	White	222—224	76	66.45 (67.35)	8.35 (8.50)
(10)	*trans*-$[RuI(CO)(dcpe)_2]BPh_4$	White	208—210	78	64.90 (65.10)	8.35 (8.25)
(14)	$[RuH(dcpe)_2]PF_6$	Red-orange	220—222	116	56.10 (57.20)	9.05 (8.95)

[a] In acetone at 22 °C, for 10^{-3} mol dm^{-3} solutions, unless otherwise stated. [b] Required values are given in parentheses. [c] In dichloromethane at 22 °C, for 10^{-3} mol dm^{-3} solutions. [d] Plots of Λ_M *vs.* the square root of the molar concentration, according to the Onsager equation $\Lambda_0 = \Lambda_M + \alpha c^{1/2}$, give Λ_0 values of 89, 98, and 94 Ω^{-1} cm^2 mol^{-1}, and α values of 480, 536, and 480 Ω^{-1} 10^{-2} dm$^{7/2}$ mol$^{-3/2}$, for complexes **(4)**, **(5)**, and **(6)**, respectively.

n.m.r. spectra of some $[RuX(L{-}L)_2]^+$ complexes have been also attributed to a square-pyramidal structure with the X ligand at the apex, and two inequivalent pairs of *trans*-phosphorus atoms in the distorted basal plane.[15]

For this reason, we have determined the crystal structure of complex (**7**) (see below): in agreement with the former interpretation of n.m.r. data, the $[RuCl(dcpe)_2]^+$ cation shows a distorted t.b.p. geometry, with two apical phosphorus atoms. The ^{31}P n.m.r. signals at *ca.* 81 and 53 p.p.m. observed for (**4**)—(**6**) can thus be assigned to equatorial and axial phosphorus atoms, respectively.[5] Probably, the presence of different groups in the equatorial plane (one chlorine and two phosphorus atoms) lowers the symmetry of (**4**)—(**6**) in such a manner that diamagnetism is achieved, while two unpaired electrons are expected for a regular t.b.p. complex of a d^6 metal ion. Recently, also a diamagnetic d^6 five-co-ordinate iridium(III) complex, $[IrMe(CH_2CMe_3)L]$ $\{L = [(Ph_2PCH_2SiMe_2)_2N]^-\}$, has been structurally characterized as t.b.p.[23]

The n.m.r. behaviour below 253 K indicates that a second process occurs at very low temperatures. In view of the well known tendency of ruthenium(II) complexes to give halide-bridged species,[1,24,25] the simplest explanation for the appearance of the two triplets on cooling solutions of (**4**)—(**6**) to 143 K is the formation of dimers such as $[\{RuX(dcpe)_2\}_2]^{2+}$, with each ruthenium atom in an octahedral six-co-ordinate environment. Nevertheless, this hypothesis appears unlikely, since the bulkiness of the dcpe ligands should inhibit such an associative rearrangement. In fact, the ^{31}P n.m.r. spectrum at 143 K of a solution containing the bromo- and iodo-derivatives (**5**) and (**6**) in a 1:1 molar ratio appears as the superimposition of the spectra of (**5**) and (**6**) at the same temperature, and there is no evidence for the formation of mixed bromo–iodo bridged species.

A possible interpretation of the observed spectral pattern is that solvation equilibrium (2) becomes important at low

$$[RuX(dcpe)_2]^+ + solv \rightleftharpoons trans\text{-}[RuX(solv)(dcpe)_2]^+ \quad (2)$$

temperature. Loss and addition of the solvent molecule, according to the dynamic equilibrium (3), may cause the

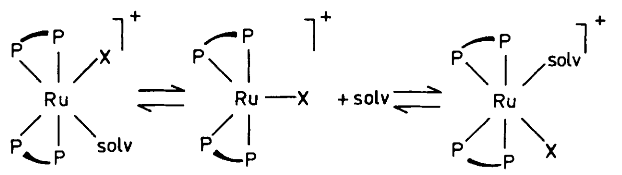

(3)

equivalence of the equatorial groups on the n.m.r. time-scale, while at this low temperature there is no scrambling of the axial and equatorial phosphorus atoms in the five-co-ordinate intermediate. The limiting spectrum is apparently not reached even at 133 K, the lowest available temperature. An analogous interpretation has been offered by Sime and Stephenson[25] for the low-temperature n.m.r. behaviour of $[RuX\{P(OMe)Ph_2\}_4]^+$. However, it should be noted that the solutions of (**4**)—(**6**) at 133 K also maintain the deep red or purple colours which are associated with five-co-ordinate species. This discounts the possibility of strong solvation, since the six-co-ordinated species formed with a solvent molecule are yellow. Other interpretations, invoking either interligand interactions or blocking of the vacant co-ordination site of complexes (**4**)—(**6**) by the bulky cyclohexyls are less precedented.

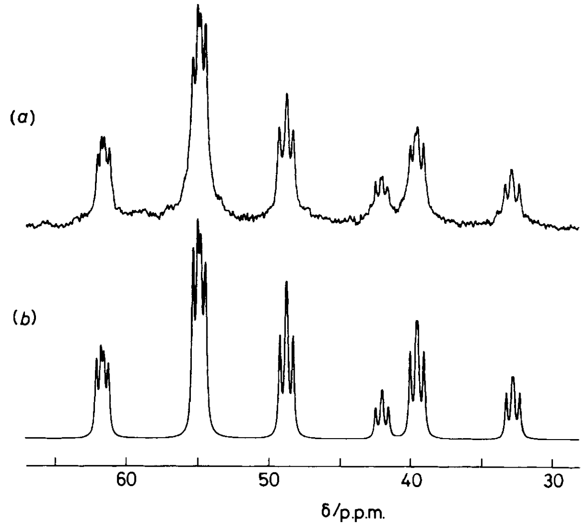

Figure 2. Experimental (*a*) and simulated ($W_{\frac{1}{2}}$ = 6.5 Hz) (*b*) ^{31}P n.m.r. spectra of $[RuI(CO)(dcpe)_2]BPh_4$ (**10**) at 153 K

Owing to their co-ordinatively unsaturated nature, complexes (**4**)—(**6**) are reactive towards a variety of ligands, although they are remarkably stable to oxygen in the solid state. On addition of excess of halide ions to dichloromethane solutions of (**4**)—(**6**), the bands of the $[RuX(L{-}L)_2]^+$ chromophores decrease, according to dissociation equilibrium (1). Spectrophotometric measurements in the presence of variable amounts of X^- show that the stability of the six-co-ordinate species decreases with increasing halide size.

Carbon monoxide readily reacts with (**4**)—(**6**) in dichloromethane solution to produce the white, six-co-ordinate derivatives *trans*-$[RuX(CO)(dcpe)_2]BPh_4$ [X = Cl (**8**), Br (**9**), or I (**10**)]. The monocarbonyl adducts are 1:1 electrolytes in acetone solution, and their i.r. mull spectra contain an intense absorption at *ca.* 1930 cm^{-1}, identifiable as a CO stretching vibration. A *trans* configuration can be assigned to complex (**8**) in view of the position of the Ru–Cl stretching frequency (280 cm^{-1}), which falls in the range expected for mutually *trans* terminal chlorine and CO.[1] Consistently with the *trans* structure, the ^{31}P-$\{^1$H$\}$ n.m.r. spectra of (**8**)—(**10**) show, at room temperature, a sharp signal at about 49 p.p.m. However, the singlets broaden when the temperature is lowered below 213 K, and the spectra at 173 K distinctly show six broad signals, which eventually sharpen into resolved multiplets at 153 K.

The low-temperature limiting spectra can be reproduced by computer simulation assuming an ABCD spin system. The calculated spectral parameters are reported in Table 2, and the experimental and simulated spectra for the iodo-derivative (**10**) are shown in Figure 2. The values of *ca.* 220 Hz found for two of the ^2J(P–P) coupling constants imply the presence of two pairs of *trans*-phosphorus atoms, thus suggesting that CO and X are still in *trans* positions. A plausible interpretation of the dynamic n.m.r. behaviour is that in these complexes the bulky cyclohexyl groups interact in such a way to destroy the C_{2v} symmetry of the molecule, and that the ligand motions are sufficiently restricted at low temperature to let the reduction of symmetry be apparent on the n.m.r. time-scale. Jesson and co-workers[26] observed a similar temperature effect in the ^{31}P n.m.r. spectra of some iron(II) six-co-ordinate complexes with $P(OR)_2Ph$ ligands.

In co-ordinating solvents such as acetonitrile or nitromethane, the dissolution of (**4**)—(**6**) occurs with the formation of yellow solutions, whose electronic spectra do not show absorptions in the visible region. The spectroscopic and conductivity data can be interpreted in terms of an equilibrium involving six-co-ordinate species, formed by addition of a solvent molecule (solv) to the vacant co-ordination site of the five-co-ordinate cations [equation (2)]. Attempts to isolate the acetonitrile or nitromethane adducts were unsuccessful, since they readily

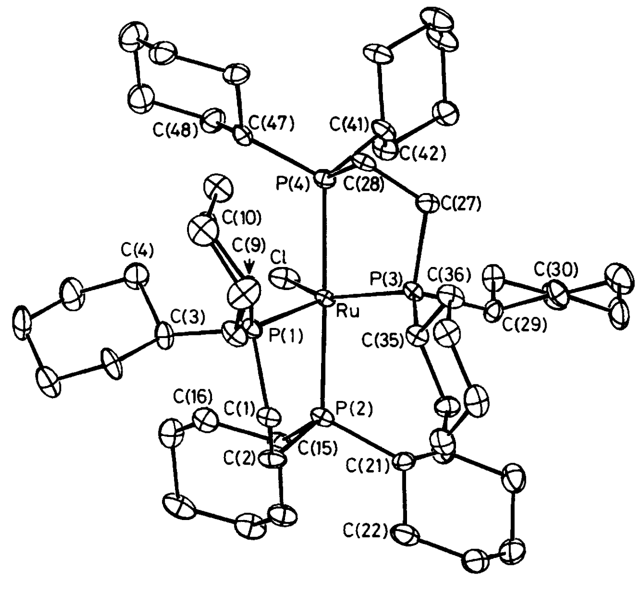

Figure 3. The molecular structure of the $[RuCl(dcpe)_2]^+$ cation

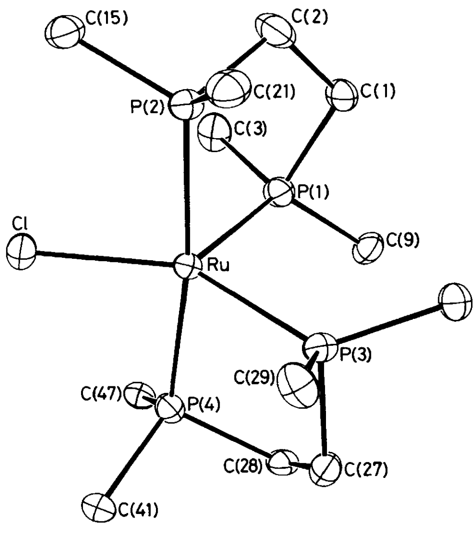

Figure 4. View of the $[RuCl(dcpe)_2]^+$ cation showing the inner co-ordination sphere

decompose in the solid state. The *trans* geometry is inferred for the adducts of (4) from the $^{31}P-\{^1H\}$ n.m.r. spectra, which show a single signal at 43.3 and 41.3 p.p.m. for acetonitrile and nitromethane solutions, respectively. We have briefly investigated the interaction between (**4**)—(**6**) and acetonitrile in solution. The i.r. spectra of the five-co-ordinate cations in dichloromethane in the presence of a stoicheiometric amount of acetonitrile show nitrile stretching absorptions in the range 2 254—2 244 cm^{-1}. The band of co-ordinated nitrile is more intense and, in contrast to almost all acetonitrile complexes, slightly shifted to lower frequencies than for the free ligand [v(CN) 2 256 cm^{-1}]. A similar decrease in the nitrile stretching frequency has been observed for acetonitrile when co-ordinated to the penta-ammineruthenium(II) cation, and has been interpreted in terms of π back bonding.[27]

The room-temperature ^{31}P n.m.r. spectra of the adducts *trans*-$[RuX(MeCN)(dcpe)_2]^+$ [X = Cl (**11**), Br (**12**), or I (**13**)] in dichloromethane–acetonitrile solutions are sharp singlets, in agreement with a *trans* formulation. However, as found for carbonyl derivatives (**8**)—(**10**), the spectra are temperature-dependent, and the singlets broaden below 213 K (CD_2Cl_2–CHF_2Cl–MeCN solution). In the case of (**12**) and (**13**) the spectra at 173 K exhibit six broad signals, which are eventually resolved in the range 153—133 K into six multiplets (ABCD spin system). The two large ^2J(P–P) values of about 240 Hz confirm the *trans* configuration of (**12**) and (**13**) (Table 2). The spectra of the chloro-derivative (**11**) display a similar temperature dependence, but a static spectrum is not reached even at 133 K. It seems probable that at very low temperatures the symmetry of (**11**)—(**13**) is lost due to the slowing down of ligand motions with respect to the n.m.r. time-scale, as previously discussed for complexes (**8**)—(**10**).

When an ethanol suspension of the hydrido complex (3) is treated with excess of NH_4PF_6 conversion into $[RuH(dcpe)_2]PF_6$ (**14**) is rapidly effected. The same product can be obtained, as a variation of the synthetic method of Ikariya *et al.*,[28] by refluxing $[RuCl_2(dmso)_4]$ and dcpe (1:2 molar ratio) in ethanol in the presence of excess of triethylamine. An orange solution is formed, from which orange crystals of (**14**) precipitate on addition of NH_4PF_6. The complex is a 1:1 electrolyte in acetone, and its i.r. spectrum shows a weak Ru–H absorption at 2 150 cm^{-1}. The n.m.r. spectra of (**14**) are temperature dependent. In dichloromethane solution at room temperature the high-field ^1H n.m.r. spectrum shows a quintet, which broadens upon cooling. At 213 K the hydride signal is a multiplet which can be described as an overlapping triplet of triplets. The room-temperature proton-decoupled ^{31}P n.m.r. spectrum exhibits a singlet at 60.1 p.p.m., which separates into two triplets at 213 K. This behaviour is close to that shown by (**4**)—(**6**), and it is possible that complex (**14**) possesses the same t.b.p. structure. It should be noted that, in spite of its co-ordinatively unsaturated character, complex (**14**) does not add acetonitrile, carbon monoxide, or dinitrogen.

Crystal Structure of Complex (**7**).—A perspective diagram of the cation is shown in Figure 3, together with the numbering; the inner co-ordination sphere is given in Figure 4, selected bond lengths and angles in Table 4. The crystal structure of (**7**) consists of closely packed, discrete $[RuCl(dcpe)_2]^+$ cations and PF_6^- anions, held together by electrostatic and van der Waals interactions. The hexafluorophosphate anion has a near-ideal octahedral geometry, with a mean P–F distance of 1.55 ± 0.03 Å.

The co-ordination geometry around the ruthenium atom is best described in terms of a trigonal bipyramid, with the bidentate dcpe ligands spanning axial and equatorial positions [P(ax) and P(eq), respectively], and the chlorine occupying the remaining equatorial position. The P(2)–Ru–P(4) angle is 173.3(1)°, in reasonable agreement with the requirements of t.b.p. geometry, and the average P(2)–Ru–X and P(4)–Ru–X angles (X = equatorial ligand) are 90.7 and 90.1°, respectively. The Ru atom is displaced by 0.075(1) Å towards P(2) from the equatorial plane formed by Cl, P(1), and P(3). While basically t.b.p., the inner co-ordination sphere is somewhat distorted from the ideal geometry. The bite angles of the chelating ligands, P(1)–Ru–P(2) and P(3)–Ru–P(4), are significantly less than 90° [82.2(1) and 83.3(1)°, respectively], and are similar to those found for other chelate diphosphines which form five-membered rings. Moreover, strong distortions are apparent within the equatorial plane: besides a nearly ideal Cl–Ru–P(1) angle of 119.1(1)°, the Cl–Ru–P(3) angle is enlarged to 147.4(1)°, while P(1)–Ru–P(3) is narrowed to 93.1(1)°. Analogous distortions have been found in several d^8 and d^7 metal complexes of the type $[MX(Ph_2PCH_2CH_2PPh_2)_2]^+$ (M = Ir, X = CO;[29] M = Ru, X = NO;[30] M = Co, X = Cl[31]).

The Ru–P(eq) distances are normal for ruthenium(II) phosphine compounds, while the Ru–P(ax) bond lengths fall at the upper end of the range found for mutually *trans*-axial P

Table 4. Selected internuclear distances (Å) and angles (°) for complex (**7**)

Ru–Cl	2.386(3)	P(1)–C(9)	1.87(1)	P(4)–C(28)	1.85(1)	Cl ··· C(15)	3.30(1)
Ru–P(1)	2.267(3)	P(2)–C(2)	1.85(1)	P(4)–C(41)	1.89(1)	Cl ··· C(16)	3.25(1)
Ru–P(2)	2.437(4)	P(2)–C(15)	1.88(1)	P(4)–C(47)	1.86(1)	Cl ··· C(42)	3.32(1)
Ru–P(3)	2.322(3)	P(2)–C(21)	1.87(1)	C(1)–C(2)	1.50(2)	C(1) ··· C(14)	3.05(2)
Ru–P(4)	2.411(4)	P(3)–C(27)	1.85(1)	C(27)–C(28)	1.53(2)	C(2) ··· C(22)	3.19(2)
P(1)–C(1)	1.86(1)	P(3)–C(29)	1.86(1)	C–C^{a,b}	1.528 ± 0.021	C(27) ··· C(36)	3.06(1)
P(1)–C(3)	1.87(1)	P(3)–C(35)	1.90(1)	P–F^{a}	1.554 ± 0.032	C(28) ··· C(52)	3.19(2)
Cl–Ru–P(1)	119.1(1)	C(1)–P(1)–C(9)	102.3(6)	Ru–P(4)–C(28)	105.2(4)	P(2)–C(21)–C(22)	118(1)
Cl–Ru–P(2)	88.1(1)	C(3)–P(1)–C(9)	109.5(6)	Ru–P(4)–C(41)	117.6(5)	P(2)–C(21)–C(26)	113(1)
Cl–Ru–P(3)	147.4(1)	Ru–P(2)–C(2)	108.5(4)	Ru–P(4)–C(47)	118.2(4)	P(3)–C(27)–C(28)	112.4(8)
Cl–Ru–P(4)	85.2(1)	Ru–P(2)–C(15)	116.6(4)	C(28)–P(4)–C(41)	98.8(5)	P(4)–C(28)–C(27)	107.5(8)
P(1)–Ru–P(2)	82.2(1)	Ru–P(2)–C(21)	116.7(2)	C(28)–P(4)–C(47)	106.8(6)	P(3)–C(29)–C(30)	117(1)
P(1)–Ru–P(3)	93.1(1)	C(2)–P(2)–C(15)	103.6(6)	C(41)–P(4)–C(47)	107.9(6)	P(3)–C(29)–C(34)	109.5(9)
P(1)–Ru–P(4)	101.8(1)	C(2)–P(2)–C(21)	104.6(6)	P(1)–C(1)–C(2)	111.0(8)	P(3)–C(35)–C(36)	115.6(9)
P(2)–Ru–P(3)	101.9(1)	C(15)–P(2)–C(21)	105.5(6)	P(2)–C(2)–C(1)	110.5(9)	P(3)–C(35)–C(40)	113.3(8)
P(2)–Ru–P(4)	173.3(1)	Ru–P(3)–C(27)	109.2(4)	P(1)–C(3)–C(4)	116(1)	P(4)–C(41)–C(42)	117.3(8)
P(3)–Ru–P(4)	83.3(1)	Ru–P(3)–C(29)	110.1(4)	P(1)–C(3)–C(8)	116(1)	P(4)–C(41)–C(46)	114(1)
Ru–P(1)–C(1)	107.8(4)	Ru–P(3)–C(35)	124.5(4)	P(1)–C(9)–C(10)	113.6(9)	P(4)–C(47)–C(48)	115.6(9)
Ru–P(1)–C(3)	112.1(4)	C(27)–P(3)–C(29)	100.6(6)	P(1)–C(9)–C(14)	116.2(9)	P(4)–C(47)–C(52)	116.8(9)
Ru–P(1)–C(9)	122.0(4)	C(27)–P(3)–C(35)	103.5(5)	P(2)–C(15)–C(16)	112.1(9)	C–C–C^{a,b}	110.7 ± 1.2
C(1)–P(1)–C(3)	100.4(6)	C(29)–P(3)–C(35)	106.1(6)	P(2)–C(15)–C(20)	116(1)		

[a] Average value. [b] Cyclohexyl rings.

atoms in these complexes.[12–14,30,32–37] The Ru–Cl distance of 2.386(3) Å is close to those found in the square-pyramidal ruthenium(II) compounds (mean 2.390 ± 0.004 Å).[12,14] The two chelate rings have similar unsymmetrical conformations, with the C atoms lying on the same side with respect to the P–Ru–P planes, and P(1)–C(1)–C(2)–P(2) and P(3)–C(27)–C(28)–P(4) torsional angles in the normal range for chelate diphosphine complexes [44(1) and 49.8(8)°, respectively].[38]

The spread in the C–P–C and Ru–P–C angles reflects both the constraints imposed by the chelate rings and the steric requirements of the bulky cyclohexyl substituents (Table 4). All the eight cyclohexyl rings are in a chair conformation, and there is no evidence of any significant interaction between the ruthenium and any cyclohexyl hydrogen atom.

Conclusions

Our results with dcpe, together with previous reports on other diphosphine derivatives,[4,5,7] clearly show that the chemistry of six-co-ordinate $[RuX_2(L\text{–}L)_2]$ appears to be very sensitive to the steric properties of the diphosphine. The tendency to dissociate, giving five-co-ordinate unsaturated species $[RuX(L\text{–}L)_2]^+$, increases with increasing ring size of the chelate in the order: six- > five- ≫ four-membered. Moreover, the dissociation becomes more facile when the size of the substituents at phosphorus is increased, as when replacing methyl with a larger group such as phenyl or cyclohexyl. Similar observations have been made also with unidentate phosphines, where five-co-ordination *vs.* octahedral geometry around the ruthenium(II) centre is preferred with bulky phosphine ligands, such as triphenylphosphine.

The $[RuX(L\text{–}L)_2]^+$ cations appear to be trigonal bipyramidal, and this contrasts with theoretical arguments which conclude that a square pyramid is favoured for d^6 five-co-ordinate species.[11] It should be noted that the $[RuX(dcpe)_2]^+$ complexes are stereochemically non-rigid, while the analogous $[RuX\{Ph_2P(CH_2)_3PPh_2\}_2]^+$ give a static ^{31}P n.m.r. spectrum at room temperature.[5] This is in accord with the observation that the barrier to intramolecular rearrangement in t.b.p. diphosphine complexes decreases when the size of the chelate ring is reduced.[22] With respect to the well known square-pyramidal $[RuX_2(PPh_3)_3]$ complexes, the t.b.p. geometry is preferred in $[RuX(L\text{–}L)_2]^+$ probably because the chelate rings introduce further steric strain, with the restriction of the possible reciprocal orientations of the $-PR_2$ groups in each diphosphine.

That considerable steric strain is present in the six-co-ordinate complexes of ruthenium(II) with dcpe is also apparent in the unusual n.m.r. behaviour of the *trans*-$[RuX(L)(dcpe)_2]^{\bullet}$ (L = CO or MeCN) derivatives. The steric hindrance of the bulky substituents at the phosphorus atoms is critical, and their motions can be slowed simply by lowering the temperature, so that the symmetry of the molecule is removed, as can be detected by ^{31}P n.m.r. spectroscopy.

Experimental

All manipulations were performed under argon with use of standard Schlenk-line techniques. Solvents were purified by standard methods. All chemicals used were of reagent grade or comparable purity. The ligand dcpe was prepared according to the method of Issleib *et al.*[39] The starting materials $[RuCl_2(dmso)_4]$,[17] $[RuCl_2(PPh_3)_3]$,[2] $[RuBr_2(dmso)_4]$,[18] $[RuH(Cl)(PPh_3)_3]$,[40] and $[RuI_2(dmso)_4]$[18] were prepared according to the literature. The complex $[RuBr_2(PPh_3)_3]$ was prepared as described by Stephenson and Wilkinson,[2] but starting from $RuBr_3\cdot3H_2O$. Yields are based on ruthenium.

Infrared and u.v.–visible spectra were recorded on DS 702 G and Uvidec 505 Jasco spectrophotometers, respectively. Proton and $^{31}P\text{-}\{^1H\}$ n.m.r. spectra were recorded on a Bruker WP 80 SY spectrometer. Spectra at temperatures lower than 173 K were run in $CD_2Cl_2\text{–}CHF_2Cl$ solutions. Positive ^{31}P chemical shifts are downfield from 85% H_3PO_4 as external standard; ^1H chemical shifts are referenced to $SiMe_4$. N.m.r. spectral simulations were performed on an Aspect 2000 computer using PANIC (Bruker Spectrospin AG). Conductance data were measured on a Metrohm E 518 conductivity bridge. Melting points (uncorrected) were obtained in capillaries sealed under argon. Microanalyses were performed by the Microanalytical Laboratory of our Institute.

Preparations.—*trans*-$[RuX_2(dcpe)_2]$ [X = Cl (**1**) or Br (**2**)]. *Method* (*a*) The ligand dcpe (0.845 g, 2.0 mmol) and $[RuX_2(dmso)_4]$ (1.0 mmol) (X = Cl, 0.484; Br, 0.573 g) were dissolved in benzene (40 cm^3), and the resulting solution refluxed for 1 h, during which the colour changed from yellowbrown to pale orange. The solution was then concentrated under vacuum, and diethyl ether (20 cm^3) was added; the pale orange or pink precipitate thus obtained was filtered off, washed repeatedly with ether, and dried under vacuum. Yields: (**1**), 90%; (**2**), 60% after recrystallization from benzene–diethyl ether.

(*b*) The ligand dcpe (0.845 g, 2.0 mmol) and $[RuX_2(PPh_3)_3]$ (1.0 mmol) (X = Cl, 0.959; Br, 1.048 g) were refluxed in benzene (40 cm^3) for 1 h, and then worked up as described in (*a*). Yields: (**1**), 85; (**2**), 60% after recrystallization from benzene–diethyl ether.

trans-$[RuH(Cl)(dcpe)_2]$ (**3**). The complex $[RuH(Cl)(PPh_3)_3]$ (0.924 g, 1.0 mmol) and dcpe (0.845 g, 2.0 mmol) were dissolved in benzene (25 cm^3). During heating under reflux (1 h), the colour of the resulting solution changed from purple-red to orange, and eventually to light yellow. After cooling to room temperature, the solution was filtered and concentrated under vacuum. Addition of hexane (20 cm^3) yielded a white precipitate, which was filtered off, washed repeatedly with ether, and dried under vacuum: yield 80%.

$[RuX(dcpe)_2]BPh_4$ [X = Cl (**4**), Br (**5**), *or* I (**6**)]. *Method* (*a*). The ligand dcpe (0.845 g, 2.0 mmol), $[RuX_2(dmso)_4]$ (1.0 mmol) (X = Cl, 0.484; Br, 0.573; I, 0.667 g), and $NaBPh_4$ (3.423 g, 10.0 mmol) were mixed in ethanol (30 cm^3) and refluxed for 1 h. Purple solutions were readily formed, from which purple crystals precipitated. After cooling, the products were filtered off, washed with ethanol, and dried *in vacuo*. Pure products were obtained by recrystallization from dichloromethane–ethanol. Yields: (**4**), 60; (**5**), 55; (**6**), 65%.

Method (*b*) [*for* (**4**) *and* (**5**)]. Instead of $[RuX_2(dmso)_4]$, $[RuX_2(PPh_3)_3]$ (1.0 mmol) (X = Cl, 0.959, Br, 1.048 g) was treated as described in (*a*). Yields: (**4**), 60; (**5**), 55%.

$[RuCl(dcpe)_2]PF_6$ (**7**). This product was obtained as described for (**4**), using NH_4PF_6 (1.630 g, 10.0 mmol) instead of $NaBPh_4$: yield 0.338 g (30%).

trans-$[RuX(CO)(dcpe)_2]BPh_4$ [X = Cl (**8**), Br (**9**), *or* I (**10**)]. Dichloromethane solutions (25 cm^3) of complexes (**4**)—(**6**) (0.5 mmol; X = Cl, 0.650; Br, 0.673; I, 0.696 g) were saturated with carbon monoxide. The solution colours turned from purple to yellow within 2 min. After filtering, ethanol (20 cm^3) was added, and the dichloromethane removed under vacuum. The resulting white precipitates were filtered off, washed with ethanol, and dried *in vacuo*. Yields: (**8**), 75; (**9**), 80; (**10**), 80%.

$[RuH(dcpe)_2]PF_6$ (**14**). *Method* (*a*). The complex *trans*-$[RuH(Cl)(dcpe)_2]$ (0.983 g, 1.0 mmol) and NH_4PF_6 (1.630 g, 10.0 mmol) were suspended in ethanol (20 cm^3) and shaken for 12 h. The resulting orange precipitate was filtered off, washed with ethanol, dried under vacuum, and recrystallized from dichloromethane–ethanol: yield 0.655 g (60%).

Method (*b*). The complex $[RuCl_2(dmso)_4]$ (0.484 g, 1.0 mmol), dcpe (0.845 g, 1.0 mmol), and triethylamine (1.4 cm^3, 20 mmol) were suspended in ethanol (30 cm^3) and refluxed for 3 h, during which the solution colour turned from yellow to orange. After addition of NH_4PF_6 (1.630 g, 10.0 mmol) dissolved in ethanol (10 cm^3) the solution was refluxed until an orange precipitate formed (1 h). After cooling, the product was filtered off, washed repeatedly with ethanol, dried under vacuum, and recrystallized from dichloromethane–ethanol: yield 0.550 g (50%).

X-*Ray Crystallography*.—Purple crystals of complex (**7**) were grown under an argon atmosphere by slow diffusion of ethanol into a dichloromethane solution of the complex.

Crystal data. $C_{52}H_{96}ClF_6P_5Ru$, M = 1 126.7, monoclinic,

Table 5. Atomic positional parameters (fractional co-ordinates), with estimated standard deviations in parentheses, for complex (**7**)

Atom	*x*	*y*	*z*
Ru	0.282 44(6)	0.220 59(7)	0.172 96(3)
Cl	0.442 1(2)	0.256 6(2)	0.203 4(1)
P(1)	0.204 8(2)	0.293 1(2)	0.101 6(1)
P(2)	0.332 0(2)	0.122 6(2)	0.107 8(1)
P(3)	0.150 1(2)	0.145 7(2)	0.188 2(1)
P(4)	0.252 5(2)	0.319 4(2)	0.241 7(1)
P(5)	−0.006 2(3)	0.249 8(3)	0.383 6(2)
F(1)	−0.072 1(7)	0.175 9(7)	0.402 3(4)
F(2)	−0.094 8(7)	0.307 6(8)	0.359 0(4)
F(3)	0.052 1(7)	0.326 1(7)	0.361 1(1)
F(4)	0.077 0(7)	0.193 9(8)	0.408 9(6)
F(5)	−0.012 2(9)	0.196 2(8)	0.332 8(4)
F(6)	−0.008(1)	0.304 6(7)	0.433 0(4)
C(1)	0.181 2(7)	0.208 1(9)	0.048 2(4)
C(2)	0.267 6(9)	0.156 7(9)	0.043 1(4)
C(3)	0.280 8(8)	0.375 4(9)	0.073 9(4)
C(4)	0.330 8(9)	0.445 5(9)	0.110 7(5)
C(5)	0.409(1)	0.493(1)	0.086 9(6)
C(6)	0.366(1)	0.535(1)	0.035 1(6)
C(7)	0.316(1)	0.467(1)	−0.001 1(5)
C(8)	0.238 4(9)	0.420(1)	0.022 1(5)
C(9)	0.088 1(7)	0.345 4(8)	0.100 2(4)
C(10)	0.092 2(8)	0.445 9(9)	0.119 7(5)
C(11)	−0.004 3(9)	0.475(1)	0.127 3(5)
C(12)	−0.074 3(9)	0.471(1)	0.077 1(6)
C(13)	−0.077 6(8)	0.375(1)	0.055 4(6)
C(14)	0.018 4(8)	0.339(1)	0.047 5(4)
C(15)	0.457 5(8)	0.131 5(9)	0.100 7(4)
C(16)	0.483 5(8)	0.229(1)	0.086 7(4)
C(17)	0.588 7(9)	0.241(1)	0.086 5(5)
C(18)	0.618 8(8)	0.169(1)	0.050 7(5)
C(19)	0.596 1(8)	0.076(1)	0.065 8(5)
C(20)	0.489 4(8)	0.065(1)	0.063 2(5)
C(21)	0.308 5(8)	−0.002 4(8)	0.112 3(4)
C(22)	0.287 9(9)	−0.058(1)	0.061 7(5)
C(23)	0.261 4(9)	−0.155(1)	0.071 5(5)
C(24)	0.333(1)	−0.201(1)	0.111 5(6)
C(25)	0.349(1)	−0.148(1)	0.162 1(5)
C(26)	0.378 8(9)	−0.051 0(9)	0.153 5(5)
C(27)	0.103 9(7)	0.205 9(8)	0.240 1(4)
C(28)	0.126 8(7)	0.308 0(8)	0.241 8(4)
C(29)	0.181 9(8)	0.033 6(8)	0.220 1(4)
C(30)	0.106 7(8)	−0.014 5(9)	0.244 6(5)
C(31)	0.143(1)	−0.106(1)	0.268 0(5)
C(32)	0.229(1)	−0.093(1)	0.310 2(5)
C(33)	0.305 3(9)	−0.046(1)	0.287 3(5)
C(34)	0.270 8(8)	0.044 8(9)	0.261 6(5)
C(35)	0.042 8(7)	0.123 9(8)	0.137 1(4)
C(36)	−0.050 7(7)	0.131(1)	0.155 9(5)
C(37)	−0.133 4(7)	0.121(1)	0.111 9(5)
C(38)	−0.126 4(8)	0.033(1)	0.084 3(5)
C(39)	−0.036 5(9)	0.025(1)	0.063 3(5)
C(40)	0.047 4(8)	0.033 3(9)	0.107 1(5)
C(41)	0.298 2(7)	0.282(1)	0.310 6(1)
C(42)	0.398 2(8)	0.250 0(9)	0.323 2(4)
C(43)	0.417 6(9)	0.205(1)	0.378 0(4)
C(44)	0.397(1)	0.271(1)	0.418 8(4)
C(45)	0.298(1)	0.307(1)	0.405 7(5)
C(46)	0.277 7(9)	0.351(1)	0.351 7(4)
C(47)	0.276 4(7)	0.443 6(8)	0.236 9(4)
C(48)	0.377 5(9)	0.472 7(9)	0.255 7(5)
C(49)	0.395(1)	0.569(1)	0.240 4(6)
C(50)	0.329(1)	0.636(1)	0.260 5(6)
C(51)	0.227(1)	0.607(1)	0.240 3(5)
C(52)	0.210 1(8)	0.509 6(9)	0.257 5(5)

$a = 14.614(3)$, $b = 14.625(3)$, $c = 26.196(3)$ Å, $\beta = 100.41(1)°$, $U = 5\,507(1)$ Å^3 (by least-squares refinement on setting angles of 25 randomly selected reflections with $24 \leqslant 2\theta \leqslant 32°$) ($\lambda = 0.710\,69$ Å), space group $P2_1/c$ (from preliminary Weissenberg and precession photographs), $D_m = 1.35$ g cm^{-3}, $Z = 4$, $D_c = 1.36$ g cm^{-3}, μ(Mo-K_α) = 5.2 cm^{-1}, $F(000) = 2\,392$, purple-red platelet of approximate dimensions $0.3 \times 0.5 \times 0.6$ mm.

Data collection. Enraf-Nonius CAD4 diffractometer, continuous ω–θ scans with ω scan width = $(1.1 + 0.35 \tan \theta)$; θ scan width = 0.5ω width, ω scan speed = 1.0—5.0° min^{-1}, graphite-monochromated Mo-K_α radiation; no statistical variation during data collection for four standard reflections monitored every 4 000 s of exposure time; 10 526 reflections measured ($3 \leqslant \theta \leqslant 27$; $-18 \leqslant h \leqslant 18$, $0 \leqslant k \leqslant 18$, $0 \leqslant l \leqslant 33$); absorption correction by the empirical ψ-scan method (minimum transmission 90.61, maximum 99.98, average 96.93%).[41] 3 219 Unique data with $I > 3\sigma(I)$ were used in the calculations.

Structure solution and refinement. Neutral atom scattering factors from the literature.[42a] Anomalous dispersion effects included in F_c using Cromer's values for f' and f''.[42b] Conventional Patterson and Fourier methods followed by full-matrix least-squares refinement, with anisotropic thermal parameters for non-H atoms. Hydrogen atoms located at calculated positions (C–H 1.0 Å), with isotropic thermal parameters $B = 1.3B_c(\text{iso})$ [B_c(iso) = isotropic equivalent thermal parameter of C atom bound to H]; their contributions, held constant, were included in the final refinement cycles. The function minimized was $w(|F_o| - |F_c|)^2$, where $w = 1/[\sigma(F_o) + (0.02F_o)^2 + 1.0]$. Refinement converged to $R = 0.052$ and $R' = 0.060$. The maximum shift/σ in final cycles including scale factor was 0.06 and the goodness-of-fit 0.914. In the final Fourier difference map the highest positive and negative peaks were 0.60 and -0.38 e Å^{-3}, respectively, in the proximity of the PF_6^- anion. All data processing was performed on a PDP 11/44 computer using the Enraf-Nonius SDP program library.[41] The final positional parameters for non-H atoms are given in Table 5.

Additional material available from the Cambridge Crystallographic Data Centre comprises H-atom co-ordinates, thermal parameters and remaining bond lengths and angles.

Acknowledgements

Support of this work by the Italian Consiglio Nazionale delle Richerche, Rome, is gratefully acknowledged. We thank Professor L. Randaccio (Dipartimento di Scienze Chimiche, Universitá di Trieste) for data collection and computing facilities, and Mr. F. Tubaro and Mr. P. Polese for technical assistance.

References

1 E. A. Seddon and K. R. Seddon, 'The Chemistry of Ruthenium,' Elsevier, Amsterdam, 1984, pp. 487—668; C. A. McAuliffe and W. Levason, 'Phosphine, Arsine, and Stibine Complexes of the Transition Elements,' Elsevier, Amsterdam, 1979.

2 T. A. Stephenson and G. Wilkinson, *J. Inorg. Nucl. Chem.*, 1966, **28**, 945.

3 P. S. Hallman, B. R. McGarvey, and G. Wilkinson, *J. Chem. Soc. A*, 1968, 3143.

4 M. Bressan and P. Rigo, *Inorg. Chem.*, 1975, **14**, 2286.

5 J. C. Briggs, C. A. McAuliffe, and G. Dyer, *J. Chem. Soc., Dalton Trans.*, 1984, 423.

6 J. Chatt and R. G. Hayter, *J. Chem. Soc.*, 1961, 896.

7 M. Bressan and A. Morvillo, *Inorg. Chim. Acta*, 1987, **132**, 1.

8 M. Bressan and P. Rigo, *J. Inorg. Nucl. Chem.*, 1976, **38**, 592.

9 T. V. Ashworth and E. Singleton, *J. Chem. Soc., Chem. Commun.*, 1976, 705.

10 B. Chaudret, G. Commenges, and R. Poilblanc, *J. Chem. Soc, Dalton Trans.*, 1984, 1635.

11 R. G. Pearson, *J. Am. Chem. Soc.*, 1969, **91**, 4947; P. R. Hoffman and K. G. Caulton, *ibid.*, 1975, **97**, 4221.

12 S. J. La Placa and J. A. Ibers, *Inorg. Chem.*, 1965, **4**, 778.

13 A. C. Skapski and P. G. H. Troughton, *Chem. Commun.*, 1968, 1230.

14 F. A. Cotton and M. Matusz, *Inorg. Chim. Acta*, 1987, **131**, 213.

15 T. V. Ashworth, A. A. Chalmers, and E. Singleton, *Inorg. Chem.*, 1985, **24**, 2125.

16 B. R. James, E. Ochiai, and G. L. Rempel, *Inorg. Nucl. Chem. Lett.*, 1971, **7**, 781.

17 I. P. Evans, A. Spencer, and G. Wilkinson, *J. Chem. Soc., Dalton Trans.*, 1973, 204.

18 J. R. Barnes and R. J. Goodfellow, *J. Chem. Res.*, (*M*) 1979, 4301.

19 B. P. Sullivan and T. J. Meyer, *Inorg. Chem.*, 1982, **21**, 1037.

20 W. J. Geary, *Coord. Chem. Rev.*, 1971, **7**, 81 and refs. therein.

21 J. R. Shapeley and J. A. Osborn, *Acc. Chem. Res.*, 1973, **6**, 305.

22 J. S. Miller and K. G. Caulton, *J. Am. Chem. Soc.*, 1975, **97**, 1067.

23 M. D. Fryzuk, P. A. MacNeil, and R. G. Ball, *J. Am. Chem. Soc.*, 1986, **108**, 6414.

24 R. A. Jones, F. M. Real, G. Wilkinson, A. M. R. Galas, M. B. Hursthouse, and K. M. Abdul Malik, *J. Chem. Soc., Dalton Trans.*, 1980, 511.

25 W. J. Sime and T. A. Stephenson, *J. Organomet. Chem.*, 1978, **161**, 245.

26 P. Meakin, E. L. Muetterties, and J. P. Jesson, *J. Am. Chem. Soc.*, 1973, **95**, 75.

27 R. E. Clarke and P. C. Ford, *Inorg. Chem.*, 1970, **9**, 227.

28 T. Ikariya, Y. Ishii, H. Kavano, T. Arai, M. Saburi, S. Yoshikawa, and S. Akutagawa, *J. Chem. Soc., Chem. Commun.*, 1985, 922.

29 J. A. J. Jarvis, R. H. B. Mais, P. G. Owston, and K. A. Taylor, *Chem. Commun.*, 1966, 906.

30 C. G. Pierpont and R. Eisenberg, *Inorg. Chem.*, 1973, **12**, 199.

31 J. K. Stalick, P. W. R. Corfield, and D. W. Meek, *Inorg. Chem.*, 1973, **12**, 1668.

32 T. V. Ashworth, M. J. Nolte, E. Singleton, and M. Laing, *J. Chem. Soc., Dalton Trans.*, 1977, 1816.

33 T. V. Ashworth, M. J. Nolte, and E. Singleton, *J. Chem. Soc., Dalton Trans.*, 1976, 2184.

34 A. R. Chakravarty, F. A. Cotton, and W. Schwotzer, *Inorg. Chim. Acta*, 1984, **84**, 179.

35 F. A. Cotton, M. P. Diebold, and M. Matusz, *Polyhedron*, 1987, **6**, 1131.

36 R. G. Ball, B. R. James, J. Trotter, D. K. W. Wang, and K. R. Dixon, *J. Chem. Soc., Chem. Commun.*, 1979, 460.

37 L. M. Wilkes, J. H. Nelson, J. P. Mitchener, M. W. Babich, W. C. Riley, B. J. Helland, R. A. Jacobson, M. Y. Cheng, K. Seff, and L. B. McCusker, *Inorg. Chem.*, 1982, **21**, 1376 and refs. therein.

38 M. C. Barrett Hall, B. T. Kilbourn, and K. A. Taylor, *J. Chem. Soc. A*, 1970, 2539.

39 K. Issleib, K. Krech, and K. Gruber, *Chem. Ber.*, 1963, **96**, 2186.

40 B. Hudson, D. E. Webster, and P. B. Wells, *J. Chem. Soc., Dalton Trans.*, 1972, 1204.

41 Enraf-Nonius Structure Determination Package (SDP), Enraf-Nonius, Delft, 1980.

42 (*a*) D. T. Cromer and J. T. Waber, in 'International Tables for *X*-Ray Crystallography,' Kynoch Press, Birmingham, 1974, vol. 4, table 2.2b; (*b*) D. T. Cromer, *ibid.*, table 2.3.1.

Received 22nd *June* 1988; *Paper* 8/02485E